Kinetic Analysis of Pausing and Fidelity of Human Immunodeficiency Virus Type 1 Reverse Transcription†

Magdalena P. Pop‡ and Christof K. Biebricher*

Max-Planck-Institute for Biophysical Chemistry, Am Fassberg, D-37077 Göttingen, Germany

Received December 21, 1995; Revised Manuscript Received February 19, 1996⊗

ABSTRACT: Human immunodeficiency virus type 1 (HIV-1) reverse transcriptase catalyzes DNA synthesis from RNA and DNA templates by a sequential mechanism. This enzyme is neither processive nor distributive but has a rather intermediate behavior; at any template position, there is a certain probability that the replica strand will be extended, which we define as extensibility. The extensibility depends on the substrate concentration, i.e. on the concentration of the cognate (and to a smaller extent of the noncognate) deoxynucleoside triphosphates, in a typical Michaelis−Menten mode. The extensibility varies from position to position in a sequence-dependent manner, being particularly low at certain sites, accordingly called pause sites. The rate and fidelity of successive incorporation of nucleotides were measured and then compared with numerical integrations of the pertinent rate equations, which were composed to describe a suitable reaction mechanism and parameterized starting with rate constants reported in the literature. We found that agreement between simulation and experiment requires two-step binding of enzyme to the template−primer. In an initial second-order step, an "outer" binary complex is rapidly formed; this is followed by a slower conformational change into an "inner" complex. During multiple rounds of nucleotide incorporation, the complex remains in the inner form; the rate-determining step for enzyme release is the reversion from the inner to the outer complex, with a standard rate constant of 0.2 s^{-1}. This rate constant may be significantly increased at pause sites. In order to match the experimental results, the standard rate constants had to be modified for pause sites. At low concentrations or in the absence of the cognate nucleotide, the site-specific misinsertion frequency, a function of the nucleotide pool bias and of the efficiency to discriminate against a noncognate nucleotide, can be determined from the dependence of extensibility on concentration of cognate and noncognate substrates. The error frequency was found to be somewhat smaller than the misinsertion frequency, because mismatches are extended less efficiently than matched base pairs.

As all retroviruses, the human immunodeficiency virus type 1 (HIV-1),[1] which causes the acquired immunodeficiency syndrome, begins its intracellular infection cycle with reverse transcription of its plus-strand RNA genome; the resulting double-stranded proviral DNA is integrated into the genome of the host to induce the persistently infected state. All three enzymatic activities required for production of the proviral DNA, i.e. RNA-directed DNA synthesis, DNA-directed DNA synthesis, and hydrolysis of the RNA strand of RNA−DNA hybrids, are apparently provided by a single enzyme, the viral reverse transcriptase (RT), a heterodimer consisting of p66 kDa and p51 kDa subunits with identical N-terminal sequences.

The mechanism of reverse transcription has been the subject of many kinetic studies in vitro. Both steady-state (Perrino et al., 1989; Ricchetti & Buc, 1990; Yu & Goodman, 1992; Bakhanashvili & Hizi, 1993) and pre-steady-state (Kati et al., 1992; Reardon, 1993; Hsieh et al., 1993; Zinnen et al., 1994) measurements using various short DNA or RNA templates have been published. The picture this extensive work offers is qualitatively consistent; quantitatively, however, there are significant differences between the reported rates, most likely due to a strong influence of sequence context or of template structure. Two important features deserve special attention, the processivity and the fidelity. Both are largely dependent on base sequence and related to one another in a way that is not fully understood.

The processivity is defined as the average number of nucleotides polymerized before the enzyme and template dissociate (Huber et al., 1989). Natural RNA and DNA sequences exhibit pausing of RT-catalyzed polymerization, leading to low processivity at certain "pause site" template positions (Klarmann et al., 1993). RT dissociates from template−primer at some of them but remains bound at others. In general, the more frequently the DNA extension is interrupted, the lower the processivity.

The fidelity (or accuracy) reflects the error level introduced into the DNA replica during reverse transcription of viral RNA; the higher the frequency of mutation, the lower the fidelity. Although an average misincorporation frequency of 2.5×10^{-4} per nucleotide (Williams & Loeb, 1992) characterizes DNA polymerization catalyzed by HIV-1 RT,

† Financial support by the Bundesministerium für Forschung und Technologie, Germany (Grant 0310248A), and Evotec Biosystems is gratefully acknowledged.

* Corresponding author: Dr. Christof K. Biebricher, Max-Planck-Institute for Biophysical Chemistry, Am Fassberg, D-37077 Göttingen, Germany. Telephone: +49 (551) 201-1442. Fax: +49 (551) 201-1435. E-mail: Biebricher@daniel.dnet.gwdg.de.

‡ Present address: Department of Immunology & Cancer Research, The Hospital for Sick Children, University of Toronto, 555 University Avenue, Toronto, Ontario, Canada M5G 1X8.

⊗ Abstract published in *Advance ACS Abstracts,* April 1, 1996.

[1] Abbreviations: Tris, tris-(hydroxyethyl)aminomethane; RT, reverse transcriptase; HIV, human immunodeficiency virus; RNase, ribonuclease.

0006-2960/96/0435-5054$12.00/0

large variations in error frequency are found at different template positions, the ones with a high error frequency being the so-called mutational "hot spots".

In this work, we address the processivity and fidelity issues by compiling the available kinetic data into a total mechanism that describes the complicated kinetics of nucleotide incorporation and misincorporation by HIV-1 RT. It is shown that the mechanism is in agreement with the measured time profiles and nucleotide dependence measurements of many consecutive incorporation cycles of reverse transcription.

MATERIALS AND METHODS

Materials

HIV-1 RT heterodimer (p66/p51) was prepared to near homogeneity from recombinant *Escherichia coli*/strain 6222 (pRT66/51, pDMI,1), kindly provided by Prof. R. Goody (Max-Planck-Institute for Molecular Physiology, Dortmund, Germany), using the described procedure (Müller et al., 1989). Protein concentration was determined by the Pierce BCA Protein Assay (Smith et al., 1985). Polymerase activity was measured as described by Restle et al. (1990). The enzyme preparation had a specific polymerase activity of about 4500 units/mg, with one unit catalyzing the incorporation of 1 nmol of TMP into acid-insoluble material in 10 min at 37 °C using poly(rA)·oligo(dT) as template. According to the experiments described in the Results, only about 20% of the protein had polymerase activity; this value was confirmed by trap experiments. From filter-binding tests, it was determined that about 35% of the protein had DNA binding capacity. DNA oligonucleotides were synthesized in an Expedite automatic DNA synthesizer from Millipore. [γ-^{32}P]ATP was supplied by Amersham. Deoxyribonucleoside triphosphates were from Pharmacia. Enzymes and other molecular biology reagents were purchased from Pharmacia, Stratagene, USB, and Boehringer Mannheim. Chemicals were from Sigma or Fluka.

Methods

RNA Preparation. RNA template was prepared by in vitro transcription from recombinant plasmid DNA and purified by gel electrophoresis followed by electroelution. DNA template for in vitro transcription was synthesized and cloned by standard procedures (Sambrook et al., 1989) into the pUC18 plasmid as expression vector. RNA transcript was sequenced according to a protocol developed by G. Strunk and S. Völker (MPI for Biophysical Chemistry, Göttingen, Germany) using the Applied Biosystems type 373A sequencer.

5′ End Labeling of DNA Oligonucleotides. To 10−20 pmol of oligonucleotide in 2 μL of 10 × phosphorylation buffer [0.5 M Tris-HCl (pH 7.6), 100 mM $MgCl_2$, and 100 mM β-mercaptoethanol] was added 5 μL of fresh [γ-^{32}P]-ATP (2 MBq, 10^5 TBq/mol), and the total volume was adjusted to 18 μL. Six units of T4 polynucleotide kinase were added, and the reaction was allowed to proceed at 37 °C for 30 min. The 5′ ^{32}P-end-labeled oligonucleotide was purified by denaturing PAGE followed by autoradiography, excision of gel bands, and elution by either soaking or electroelution. In the end, 30−50 μL of stock solution of 5′-labeled DNA oligonucleotide in water was obtained with a specific activity of 2×10^3 to 2×10^4 Bq/μL.

RNA Folding. Optimal secondary structure of oligonucleotides was calculated by the method of Zuker and Stiegler (1981) using programs of the Genetics Computer Group (GCG) Sequence Analysis Software package.

Enzyme Assays. The final buffer for the assays contained 50 mM Tris-HCl (pH 8.3), 80 mM KCl, 10 mM $MgCl_2$, 1 mM dithiothreitol, 400 nM template−primer (35 Bq/μL ^{32}P), 0.08 unit/μL reverse transcriptase, and variable dNTP concentrations depending on the kind of assay. Template was annealed to primer (in 0.02 M sodium acetate solution) through mixing, heating for 3 min at 95 °C, and then incubation at 37 °C for about 1 h. RT [freshly diluted in 50 mM Tris-HCl (pH 8.3)] was then added to give a volume of 25 μL "premix" and incubation continued for another 5 min at 37 °C. Time courses were started by addition to the premix 25 μL start mix (2 × RT−buffer and 100 μM dNTP, unless otherwise stated), incubation at 37 °C, and quenching of 5 μL reaction time points in 5 μL of denaturing loading buffer (10 mM ethylenediaminetetraacetic acid, 1 mg/mL Xylene Cyanol FF, 1 mg/mL Bromphenol Blue in formamide) with shock freezing. For concentration dependence measurements, distinct start mixtures were prepared, containing 2 × RT−buffer, 100 μM pretarget site dNTP(s), and different concentrations of the dNTP to be incorporated at the target site. Each start mix received one volume premix, and each reaction was quenched after 1 min. The RT−buffer [50 mM Tris-HCl (pH 8.3), 80 mM KCl, 10 mM $MgCl_2$, and 1 mM dithiothreitol] was prepared as 5 × stock solution, sterile filtrated, and stored at −20 °C.

Product Analysis. Reaction products were resolved by polyacrylamide (12%) gel electrophoresis (60 cm × 20 cm × 0.4 mm gels) in electrophoresis buffer (100 mM Tris, 100 mM boric acid, and 1 mM ethylenediaminetetraacetic acid) under strongly denaturing conditions (7 M urea, 2500 V). Quantitative analysis was performed by autoradiography (using DuPont X-Ray CRONEX films with overnight exposure at −70 °C) followed by cutting out bands and scintillation counting in a Packard Tri-Carb 1900CA Liquid Scintillation Analyzer or by phosphorimaging using a Molecular Dynamics SF Phosphorimager and the ImageQuant software.

RESULTS

Pausing of Reverse Transcription. In this study, RNA and DNA templates with identical sequences predicted to form a hairpin loop secondary structure were used; the templates and the oligodeoxynucleotide primers used are shown in Figure 1. Extensive quantitative measurements were made only with RNA template.

Nucleotide incorporation by the DNA polymerase activity of RT was investigated by measurement of 3′ terminal extension of 5′ ^{32}P-labeled primers annealed to the template. (In the following, template always means a primer−template complex.) A high excess of template over enzyme was used. The products corresponding to different reaction times were resolved according to chain length by denaturing polyacrylamide gel electrophoresis (Figure 2) and quantified.

Extension bands of different intensities were seen. The intensities increased continually with incubation time, but after a short equilibration period, coherent growth was observed. Unequal distribution of extension products has been generally observed in nucleic acid polymerization (Mills

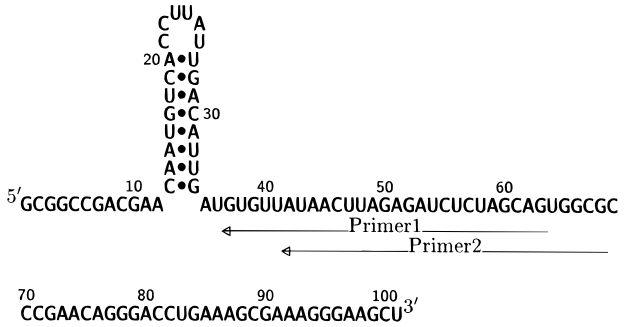

FIGURE 1: Templates and primers used. Shown is the sequence of the 101-base long RNA template predicted to form a stable hairpin loop secondary structure near the 5′ end. Bases 54 through 97 belong to the HIV-1 genome but have no direct relevance to this study. The rest of the sequence was designed to contain the hairpin but was otherwise arbitrarily chosen; the ends resulted from the cloning procedure. Structural features other than the stem-loop involving positions 13−34 are not shown. Control experiments were performed with a 63-base long DNA template homologous to the 5′ end of the RNA. As depicted, complementary oligodeoxynucleotide primers 27 bases in length were used. The measurements presented have been mainly done with primer 1. Primer 2 was used in an additional set of experiments to test the consistency of results obtained with primer 1.

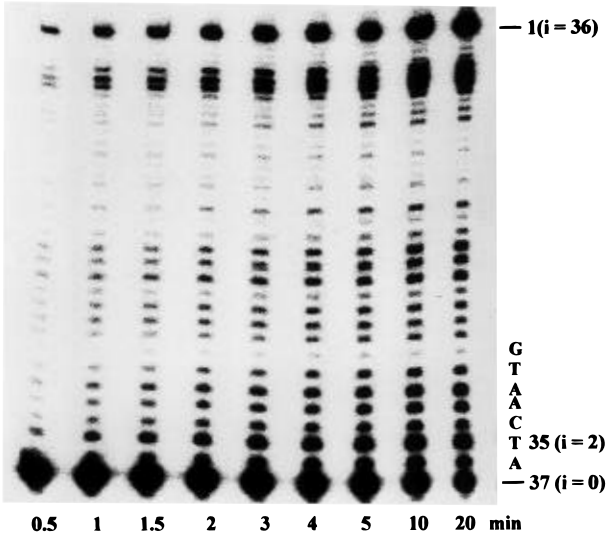

FIGURE 2: RT-catalyzed RNA-directed extension of primer 1 with 50 M of each dNTP. The reaction mixture was incubated for the indicated times, resolved by polyacrylamide gel electrophoresis, and subjected to phosphorimaging. Site-specific variation in extension is apparent from the variation in intensity of different extension intermediates. The 3′ end of the primer (position 37), the first seven cognate nucleotides that are added, as well as the template terminus (position 1) are indicated at the right; corresponding *i* values (see text) are also given. As suggested by the relative intensity of individual bands, pausing is most pronounced at position 35; this effect has been further examined here. Another strong pause effect, visible toward the end of the template (positions 7−10), has not been further pursued.

et al., 1978; Aivazashvili et al., 1981; Huber et al., 1989). For processive DNA and RNA polymerases, i.e. for polymerases which fall off only at the end of the template, this can be attributed to the variation of the nucleotide incorporation rate along the template. The situation is more complicated for RT because its DNA polymerase activity is neither processive nor distributive, the latter meaning that the enzyme falls off after each nucleotide incorporation and must rebind to continue extension. To describe the intermediate behavior of RT, a processivity has been defined as the average number of bases incorporated per encounter of the enzyme with the template (Huber et al., 1989). However, whereas this definition may be satisfactory for reverse transcription of homopolymeric templates, it does not seem adequate in the case of natural templates, because significant variation of processivity occurs from position to position due to the influence of sequence context. At each position located *i* bases downstream from the 3′ end of the primer (i.e. after *i* bases have been incorporated), the enzyme either continues extension by incorporating a nucleotide, with the rate ${}^{i}k_{\mathrm{inc}}$, or aborts extension by dissociating from the template, with the rate ${}^{i}k_{\mathrm{off}}$ (cf. definitions listed in Table 1). A quantity called "termination probability" has been proposed to describe the site-specific variation in extension (Abbotts et al., 1993; Klarmann et al., 1993); it is calculated as ${}^{i}c/({}^{i}c + {}^{\hat{}}c)$, where ${}^{i}c$ is the concentration of extension products terminating at position *i* and ${}^{\hat{}}c$ is the total concentration of all extension products ending downstream from that position, assuming "single-hit conditions" as explained later. Because in general the intensity of a band also depends on the probability of restart at that position, we prefer a related notion corresponding to a specific processivity that we will call extensibility, ${}^{i}X = {}^{\hat{}}c/({}^{i}c + {}^{\hat{}}c)$. It follows that the probability of reaching position *i* can be calculated as $\prod_{j=1}^{i} {}^{j}\mathrm{X}$, if we start counting the positions from the 3′ end of the primer. Thus, from the probability to reach full length product (0.262, $i = 36$; see Figure 2), we calculated an average $\bar{X} = 0.96$ corresponding to an average processivity $(1 - \bar{X})^{-1} = 27$. In agreement with the results of Klarmann et al. (1993), we found that these quantities are generally dependent on the template site (and structure) but independent of the primer positioning.

Bands of higher intensity are seen at pause sites, where ${}^{i}X < \bar{X}$. In Figure 2, a pause site with an *X* value of 0.84 was found at position 35. The term pausing seems to imply a temporal arrest of the polymerization. However, pausing at a certain position can be caused by a low rate of nucleotide incorporation, a high rate of dissociation of the enzyme from the template, and/or a low rate of enzyme rebinding. The contribution of the last process to pausing can be readily estimated by following the time dependence of the ${}^{i}X$ values. In the experiment shown in Figure 2, the ${}^{i}X$ values ($i \neq 0$) were time-independent until about half of the primer has been extended; thus, the influence that enzyme restart has on the extensibility could be neglected under these conditions.

Pausing at template position 35 was examined more closely by using a primer ending at position 37 (primer 1, Figure 1) and preventing extension from proceeding beyond position 31 by omission of dGTP; hence, the pause site corresponds to $i = 2$. Figure 3a shows the gel electropherogram and the time-dependent concentration profiles obtained with 50 μM dATP, 50 μM dTTP, and 5 μM dCTP. During the first 2 min, the intermediates and final products accumulated almost linearly. At longer incorporation times (>5 min, not shown in the figures), the intermediate concentrations peaked and then decreased due to rebinding of enzyme and further extension.

Assuming that ${}^{i}k_{\mathrm{inc}}$ depends on the nucleoside triphosphate concentration while ${}^{i}k_{\mathrm{off}}$ does not, the substrate dependence of ${}^{2}X$ could be examined by varying the concentration of the correct substrate, dCTP, to be incorporated at the pause site. Figure 4a shows extension profiles after 1 min in the

Table 1: Definitions

${}^{i}k_{inc}$	composite rate constant for nucleotide incorporation at position *i*	(s^{-1})
${}^{i}k_{off}$	composite rate constant for enzyme dissociation at position *i*	(s^{-1})
${}^{i}X$	extensibility; probability for extension to occur at position *i*	
${}^{i}X_{max}$	maximum extensibility at position *i*	
$\bar{X}$	average extensibility over a position range	
$(1-\bar{X})^{-1}$	processivity; average number of nucleotides incorporated during a single encounter between enzyme and template	
${}^{i}K_{x}$	dNTP substrate concentration for half-maximum extensibility at position *i*	(μM)
${}^{i}_{N}m$	discrimination coefficient; proportion of incorporation of the cognate nucleotide compared to that of the noncognate nucleotide N at position *i*	
${}^{i}_{N}f$	misinsertion frequency; probability of incorporation of the noncognate nucleotide N at position *i*	
${}^{i}f$	overall misinsertion frequency; probability of incorporation of any noncognate nucleotide at position *i*	
${}^{i}\epsilon$	error frequency; probability of finding an incorrect nucleotide at position *i* among full length products	
$1-{}^{i}\epsilon$	fidelity; probability of finding the correct nucleotide at position *i* among full length products	

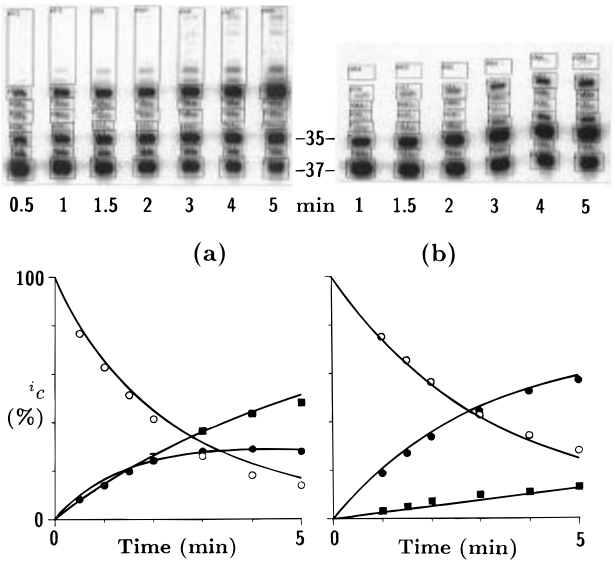

FIGURE 3: Successive nucleotide additions at the end of primer 1. Five-minute time courses are shown as resolved by polyacrylamide gel electrophoresis (upper part; phosphorimage) and as quantified data (lower part). Represented is the relative amount of DNA strands terminated at position *i* as a percentage from all extended and unextended primers present at the given time point. The experimental results are shown as symbols, whereas the continuous lines correspond to the results from the simulations using the mechanism from Figure 6 and the rate constants from Tables 2 and 3. Symbols are as follows: (○) $i = 0$, position 37; (●) $i = 2$, position 35; (■) $i > 2$, position 34 and beyond. (a) Extension of primer 1 in the presence of the cognate base for position 34, i.e. with 5 μM dCTP, 50 μM dATP, and 50 μM dTTP. Although the extension beyond position 31 was prevented by omission of dGTP, considerable misinsertion was observed. (b) Extension in the absence of the cognate base for position 34, i.e. with 50 μM dATP and 500 μM dTTP.

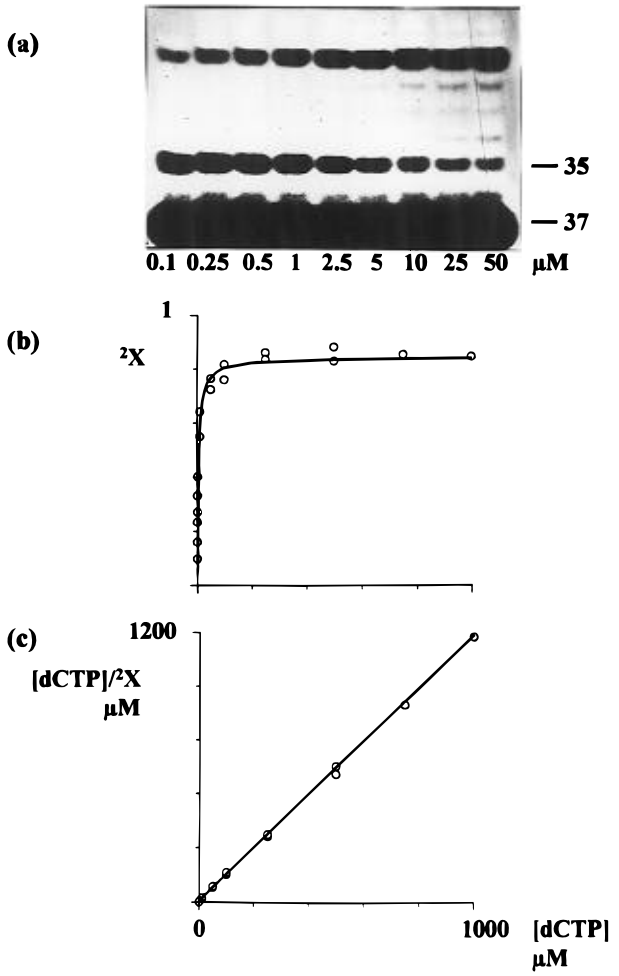

FIGURE 4: Extensibility at the pause site. (a) Primer 1 extension profiles (autoradiogram) obtained under "single-hit conditions" in the presence of 50 μM dATP, 50 μM dTTP, and variable dCTP concentrations, as indicated. (b) The extensibility at the pause site as a function of dCTP (cognate nucleotide) concentration. (c) The linearized (Hanes−Woolf) representation of data from panel b. Experimental points are shown by symbols (○) and simulations by the continuous line. The calculated values of the Michaelis−Menten parameters are as follows: ${}^{2}_{C}X_{max} = 0.84$ and ${}^{2}_{C}k_{x} = 4.6$ μM.

presence of 50 μM dATP, 50 μM dTTP, and various dCTP concentrations. During this incubation time, single-hit conditions prevailed, where each enzyme molecule encounters many template molecules while each primer is extended by a single enzyme molecule (Boosalis et al., 1987; Goodman et al., 1993).

The ${}^{2}X$ values calculated from experiments as shown in Figure 4a are plotted against dCTP concentration in Figure 4b. At low dCTP concentrations, ${}^{2}X$ increases linearly; at higher dCTP concentrations, the rate of increase of ${}^{2}X$ slows and finally reaches a maximum value, ${}^{2}_{C}X_{max}$, suggesting Michelis−Menten behavior. (The C subscript denotes *X* values pertaining to incorporation of the correct C nucleotide; a T subscript is introduced below to denote *X* values for misincoporation of T nucleotides.) Indeed, the quite good linearity of the Hanes−Woolf plot (apart from deviations at very small substrate concentrations) confirms a wide range of conditions where the Michaelis−Menten formula ${}^{2}X = {}^{2}X_{max}[S]/({}^{2}K_{x} + [S])$ holds (Figure 4c). Thus, we were able to derive values for ${}^{2}_{C}X_{max}$ and (in analogy to K_m) for ${}^{2}_{C}k_{x}$, the dCTP concentration at which ${}^{2}_{C}X$ reaches half of its maximum value. Similar measurements at the positions preceding the pause site demonstrated that the dATP and

dTTP concentrations used (50 μM) ensured maximum values of ${}^0X$ and ${}^1X$. At [dNTP] $\ll {}^iK_x$, the extensibility is linearly dependent on substrate concentration with ${}^iX = ({}^iX_{max}/{}^iK_x)$ [dNTP]; hence, ${}^iX_{max}/{}^iK_x$ is proportional to ${}^ik_{inc}$.

Misinsertion during Reverse Transcription. When the concentration of the cognate substrate for a given position is low compared to the concentrations of the noncognate ones, misinsertion, i.e. incorporation of noncognate nucleotides, cannot be neglected. This is clearly reflected by the extension pattern obtained with 50 μM dATP and 500 μM dTTP and in the absence of dCTP (Figure 3b); the extension beyond the pause site could be explained only by misinsertion, since effects of dCTP present as impurity in the dTTP solution could be ruled out. (Use of different batches of high-performance liquid chromatography (HPLC)-purified dNTPs did not change the misinsertion frequency; furthermore, the incorporation pattern showed characteristic mismatch extension behavior.) Thus, biased nucleotide pools have both mutagenic and pausing effects, and kinetic analysis of pausing cannot disregard the effects of misinsertion.

We also measured the dependence of ${}^2X$ on dTTP concentration in the absence of dCTP and derived values for ${}^2_TX_{max}$ and ${}^2_TK_x$ (Figure 5). As expected, ${}^2_TX_{max} < {}^2_CX_{max}$ and ${}^2_TK_x > {}^2_CK_x$. If we neglect contributions by dATP, the misinsertion frequency ${}^2f$ is equal to ${}^2_Tf$, i.e. the probability of incorporation of a T at this position, and is of course 1 when dCTP is absent. When both dCTP and dTTP are present, direct observation of misinsertion is not possible, because denaturing gel electrophoresis separates products according to lengths, irrespective of sequence differences. However, a discrimination coefficient ${}^2_Tm$ could be estimated from

$$ {}^2_Tm = \frac{{}^2_Ck_{inc}}{{}^2_Tk_{inc}} = \frac{{}^2_CX_{max}/{}^2_CK_x}{{}^2_TX_{max}/{}^2_TK_x} $$

(Fersht, 1985; Goodman et al., 1993). In the absence of dCTP, incorporation of dTMP at position 34 ($i = 2$) was strongly preferred over that of dAMP or dGMP; we thus neglected the contributions of ${}^2_Am$ and ${}^2_Gm$ to the overall misinsertion frequency at this position. When the pool bias between dTTP and dCTP was not extreme, the contribution by misinsertion to the total incorporation could be neglected and the misinsertion frequency

$$ {}^2f \approx {}^2_Tf = \left(1 + {}^2_Tm\frac{[\text{dCTP}]}{[\text{dTTP}]}\right)^{-1} $$

was estimated from ${}^2f \approx {}^2_Tm^{-1}$[dTTP]/[dCTP].

However, the fidelity at a given position, defined as the probability of finding the correct nucleotide at this position among all full length transcripts, is only partly determined by the single-position misinsertion frequency. Base mispairs formed by misinsertion are further discriminated against at subsequent incorporation steps. Some strands containing misinsertions are extended to full length products much later or not at all, i.e. the error frequency ${}^i\epsilon < {}^if$. Therefore, a thorough analysis of fidelity ($1 - {}^i\epsilon$) required a more detailed kinetic mechanism, including the incorporation of the next nucleotides.

Mechanism of Reverse Transcription. The mechanism of reverse transcription has been studied by several groups (Kati et al., 1992; Reardon, 1993; Hsieh et al., 1993; Zinnen et al., 1994), mainly by pre-steady-state measurements. In these experiments, identification of the intermediates formed during a single nucleotide incorporation was not possible; therefore, conclusions about the properties of these intermediates had to be drawn from indirect mechanistic arguments. While the results obtained by these groups agree on the general mechanism and the rate-determining steps, the differences between the rate constants reported are often too large to be explained by the limited accuracy of the experimental method. The rates clearly depend on the sequence context, which was different in each of these studies.

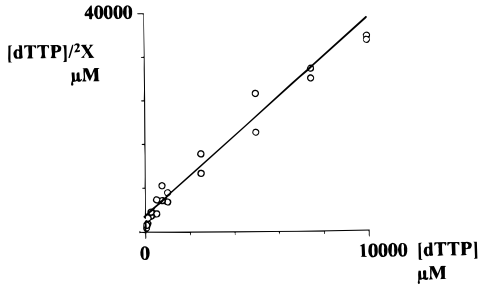

FIGURE 5: Extensibility at the pause site in the absence of dCTP. The linearized (Hanes−Woolf) representation of extensibility as a function of dTTP concentration is shown. The symbols (○) correspond to the experimental results, whereas the continuous line was obtained by simulation. The calculated values of the Michaelis−Menten parameters are as follows: ${}^2_TX_{max} = 0.28$ and ${}^2_TK_x = 830$ μM.

We compared experiments as those presented in Figures 3−5 with results of a numerical integration of the rate equations that describe the multistep incorporation reaction. Since it would be an impossible task to identify all elementary steps of a reaction as complicated as the reverse transcription, we sought instead a schematic mechanism that would adequately describe our experimental data and those published by other groups. For most rate constants, we used values reported in the literature; since these values vary from position to position, we did not attempt to obtain rate constants by fitting individual experiments but focused instead on the essential features of the extension profiles in order to reconcile the different experimental results. The computer program enabled us to use the concentration values at the end of one simulation as initial values for another run; we could thus mimic changes of conditions during a single experiment, e.g. addition of nucleotides after preincubation of enzyme and template.

The reverse transcription mechanism must include binding of the enzyme to the template, complexation of the appropriate dNTP, phospho diester formation, and liberation of pyrophosphate. The rate-limiting step during the incorporation of a single nucleotide (single turnover) was identified as a unimolecular process following substrate complexation and preceding the chemical step, which presumably represents a conformational change of an "inactive" ternary complex into an "active" one (Kati et al., 1992; Hsieh et al., 1993). On the other hand, dissociation of the enzyme from the extended product (${}^ik_{off}$) was rate-limiting during the multiple turnover reaction (Hsieh et al., 1993). Making use of these findings, we started to build our model by considering that successive incorporation of more than one nucleotide does not proceed as a simple repetition of a closed reaction cycle; rather, after each incorporation event, the enzyme−

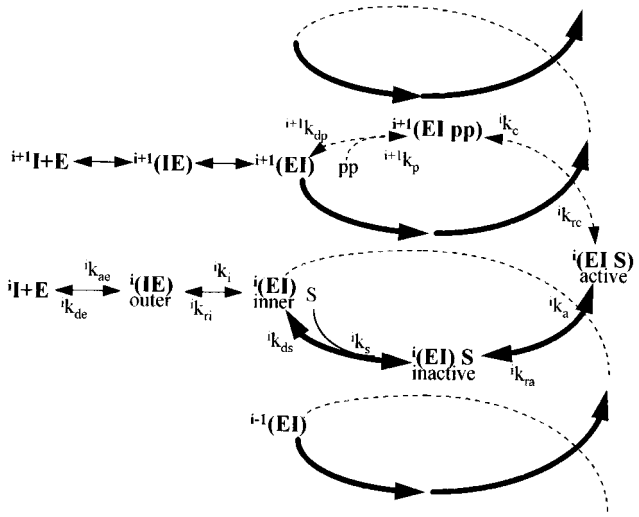

FIGURE 6: Mechanism of reverse transcription. Successive nucleotide incorporations are depicted like turns of a spiral, the *i*th turn corresponding to the *i*th incorporation cycle. Every next position is reached during the phospho diester bond formation. The standard rate constants are as defined in Table 2. Molecular species involved within one incorporation cycle are as follows: ^{i}I, free template with primer ending at position *i*; E, free enzyme; ^{i}(IE), outer binary complex at position *i*; ^{i}(EI), inner binary complex at position *i*; S, dNTP substrate added at position *i*; ^{i}(EI)S, inactive ternary complex at position *i*; ^{i}(EI S), active ternary complex at position *i*; $^{i+1}$(EI pp), pyrophosphate ternary complex at position $i + 1$; and pp, pyrophosphate. As suggested by this scheme, it is their location outside and inside the incorporation cycle that led to the naming of the two binary complexes as outer and inner, respectively. Although misinsertions were also considered in the simulations, they are not shown in this scheme. Not shown also are the decomposition of the inner binary complex and that of the inactive ternary complex with the rates $^{i}k_{\mathrm{li}}$ and $^{i}k_{\mathrm{lt}}$, respectively.

template complex arrives at a state that is equivalent but not identical to the one preceding that incorporation cycle. Therefore, we visualized the successive incorporation of nucleotides like a spiral, with entry and leaving points corresponding to enzyme binding to and release from the template, respectively (Figure 6).

However, when the published mechanism and the reported rate constants were used to simulate the successive incorporation of several nucleotides, it was impossible to reconcile the calculations with the experiments; the calculated extensibilities were too high. The discrepancy was resolved by subdivision of the enzyme−template binding (Divita et al., 1993; Rittinger et al., 1995) into a fast second-order reaction which results in a complex we may call the "outer" complex (because it is outside of the spiral) and a subsequent first-order reaction wherein the outer complex is converted into an active, "inner" complex. When we included these steps in the multi-incorporation mechanism, we had to decide in which of these two states the enzyme−template complex will arrive after addition of one nucleotide. By comparing the extension patterns obtained experimentally with the calculated ones, we found that after the completion of an incorporation cycle the binary complex remains in its inner form and does not need to undergo an activation to be further extended. It resulted therefore that $^{i}k_{\mathrm{off}}$ is a composite rate that is limited by the conformational change reverting the inner complex to the outer one ($^{i}k_{\mathrm{ri}}$, see Figure 6). However, the rate constant reported for this step, 0.01−0.04 s^{-1} (Rittinger et al., 1995), was compatible neither with published steady-state single-nucleotide incorporation measurements (Hsieh et al., 1993) nor with our experiments; we obtained good agreement with our experiments, as well as with other kinetic data, by using $^{i}k_{\mathrm{ri}} = 0.2$ s^{-1}, resulting in an $^{i}k_{\mathrm{off}}$ rate constant of 0.11 s^{-1}, consistent with published results.

The extended mechanism depicted in Figure 6 was able to adequately describe all experiments presented here as well as most kinetic experiments reported previously by other groups. The rate constants used, together with their standard values, are listed in Table 2; some of these values had to be modified at certain positions, as noted earlier, to describe pausing. This holds in particular for the pause site at position 35, as we tried to obtain the closest fit to the time profiles and the substrate dependence measurements shown in Figures 3−5. Considering the large number of parameters, it would of course be possible to generate more than one simulation in agreement with the experiments using distinct sets of rate constants. These sets, however, would have to be very similar ones because the actual number of parameters was reduced by the following constraints. (i) A sensitivity analysis, which revealed the impact changes of rate constants have on the calculated extension pattern, indicated little influence of the fast phospho diester formation and pyrophosphate release steps when the pyrophosphate concentration is low. (ii) The two second-order reactions leading to complex formation, i.e. formation of the (outer) binary complex and of the (inactive) ternary complex, were, at the time periods examined, very close to equilibrated; therefore, they contributed only through their equilibrium constants as was pointed out also by Rittinger et al. (1995). Thus, the data shown in Figures 3−5 suffice to determine an unequivocal, if not completely unique, set of rate constants that fit all experiments. Site-specific rate constants deviating from the standard ones in Table 2 are listed in Table 3.

Site-Specific Error Rates. The experiments performed with low amounts of correct substrate permitted fitting of fidelity parameters. However, attempting to fit the parameters for every position of the sequence would make the determination of the pertinent rate constants a difficult task; we therefore concentrated on those positions where experiments in the absence of the correct substrate showed a high degree of read-through, indicating particularly low fidelity. By using sufficiently high concentrations of correct nucleotides for all positions other than the target site, misinsertion could be evaluated at a specific site. As an important factor contributing to fidelity, the discrimination against mismatch extension also had to be considered; the rate constants we used for mismatch extension were derived from values reported in the literature (Zinnen et al., 1994). As seen in Figures 3−5, the rate constants we used (Table 3) fitted the experimental extension profiles well. However, we cannot exclude the possibility that other sets of rate constants for mismatch extension give comparable agreement with the experimental data, since we had no direct information on the substrate dependence of mismatch extension from our results.

Assuming that the mechanism (Figure 6) and rate constants (Tables 2 and 3) describe the mutagenic process correctly, quantitative fidelity parameters were derived from the simulations. Since at low pyrophosphate concentrations nucleotide incorporation is essentially irreversible, $^{2}k_{\mathrm{inc}}$ could be determined from the flow through the incorporation cycle at $i = 2$. A relatively low value for the discrimination

Table 2: Standard Reaction Rate Constants

${}^{i}k_{ae}$	rate constant for enzyme−template binding at position *i*	1×10^{8} M^{-1} s^{-1}
${}^{i}k_{de}$	rate constant for dissociation of outer complex at position *i*	10 s^{-1}
${}^{i}k_{li}$	rate constant for decomposition of inner complex at position *i*	10^{-3} s^{-1}
${}^{i}k_{lt}$	rate constant for decomposition of inactive ternary complex at position *i*	2 s^{-1}
${}^{i}k_{i}$	rate constant for conversion from outer to inner binary complex at position *i*	0.5 s^{-1}
${}^{i}k_{ri}$	rate constant for conversion from inner to outer binary complex at position *i*	0.2 s^{-1}
${}^{i}k_{s}$	rate constant for dNTP substrate binding at position *i*	1×10^{8} M^{-1} s^{-1}
${}^{i}k_{ds}$	rate constant for dNTP substrate dissociation at position *i*	1×10^{3} s^{-1}
${}^{i}k_{a}$	rate constant for conversion from inactive to active ternary complex at position *i*	15 s^{-1}
${}^{i}k_{ra}$	rate constant for conversion from active to inactive ternary complex at position *i*	0.06 s^{-1}
${}^{i}k_{c}$	rate constant for phospho diester bond formation at position *i*	100 s^{-1}
${}^{i}k_{rc}$	rate constant for pyrophosphorolysis at position *i*	20 s^{-1}
${}^{i}k_{p}$	rate constant for pyrophosphate binding at position *i*	1×10^{7} M^{-1} s^{-1}
${}^{i}k_{dp}$	rate constant for pyrophosphate release at position *i*	7.2×10^{4} s^{-1}

Table 3: Rate Constants Deviating from Standard[a]

rate constant	standard	primer 1	primer 2
${}^{2}k_{ri}$	0.2	1.2	3
${}^{4}k_{ri}$	0.2	0.2	0.5
${}^{2}_{C}k_{s}$	1×10^{8}	2×10^{7}	2×10^{8}
${}^{2}_{T}k_{s}$	1×10^{8}	5×10^{5}	2×10^{6}
${}^{2}_{A}k_{s}$	1×10^{8}	5×10^{4}	2×10^{5}
${}^{3}_{T}k_{s}$	1×10^{8}	7×10^{6}	5×10^{7}
${}^{3}_{A}k_{s}$	1×10^{8}	2.5×10^{6}	2×10^{6}
${}^{4}_{T}k_{s}$	1×10^{8}	5×10^{7}	2×10^{6}
${}^{4}_{A}k_{s}$	1×10^{8}	2×10^{7}	1×10^{7}
${}^{2}_{C}k_{a}$	15	10	30
${}^{2}_{T}k_{a}$	15	0.7	5
${}^{2}_{A}k_{a}$	15	0.02	0.03
${}^{3}_{T}k_{a}$	15	7	15
${}^{3}_{A}k_{a}$	15	0.5	0.5
${}^{4}_{T}k_{a}$	15	12	2
${}^{4}_{A}k_{a}$	15	5	1

[a] Units like in Table 2.

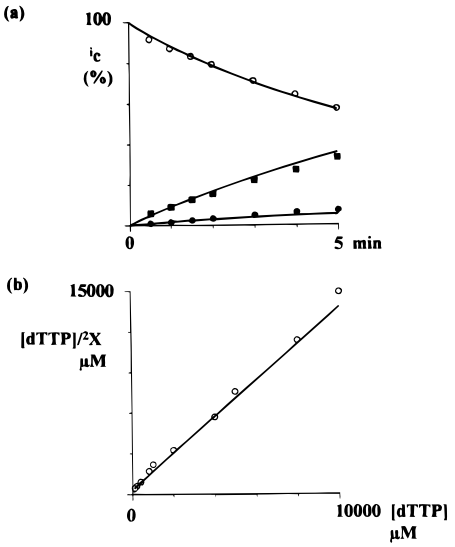

FIGURE 7: Primer 2 extension profiles. The experiments were similar to those shown in Figures 3−5. Symbols correspond to experimental results, whereas continuous lines were obtained by simulation using the mechanism from Figure 6 and the rate constants from Tables 2 and 3. (a) Shown as quantified data is a 5 min time course in the presence of the cognate base for position 39 (see Figure 1), i.e. with 5 μM dCTP and 50 μM dATP. Quantification was done as explained in the legend to Figure 3. Symbols are as follows: (○) $i = 0$, position 42; (●) $i = 2$, position 40; (■) $i > 2$, position 39 and beyond. (b) Extensibility at position 40 in the absence of dCTP. The linearized (Hanes−Woolf) representation of extensibility as a function of dTTP concentration is shown. The calculated Michaelis−Menten parameters are as follows: ${}^{2}_{T}X_{max} = 0.73$ and ${}^{2}_{T}K_{x} = 190$ μM. Not shown are the time course in the absence of dCTP as well as the dependence of ${}^{2}X$ on the dCTP concentration (${}^{2}_{C}X_{max} = 0.94$ and ${}^{2}_{C}K_{x} = 0.4$ μM).

coefficient was determined, i.e. ${}^{2}_{T}m = 560$; the dependence of misinsertion frequency on pool bias proved to be correctly predicted by the equation given above. The error frequency at the pause site appeared to be determined mainly by the misinsertion frequency; the discrimination by mismatch extension contributed about 20% to the error frequency.

Modeling of Reverse Transcription. To test the generality of the conclusions drawn from the analysis at position 35, we made a similar set of experiments with a primer ending at position 42 (primer 2; Figure 1); weaker pausing was observed at sites 40 ($i = 2$) and 38 ($i = 4$). We could describe the new experimental measurements well (Figure 7) using the same mechanism (Figure 6) and the parameters listed in Tables 2 and 3. We observed faster incorporation in this region and thus had to duplicate the rate constant of ternary complex activation (${}^{i}k_{a}$) for 1−3 and 5, as well as ${}^{2}k_{s}$ in order to account for the data obtained experimentally. Pausing at position 40 was fitted by a 20-fold increase of ${}^{2}k_{ri}$. The discrimination coefficient ${}^{2}_{T}m$ at this position was 560, the same low value as found for position 35.

The reaction model does not consider any influence of the RNase H activity of the RT. Since DNA polymerization and RNA degradation by RNase H may proceed simultaneously (Gopalakrishnan et al., 1992), some effect can be expected. Indeed, we observed effects that we could not explain with our reaction model. At late times, the polymerase activity in the experiments was observed to slow. For incubations longer than 10 min, the simulated concentrations of the unextended primers were lower and those of the paused intermediates higher than in the experiments. We examined possible influences of enzyme denaturation or binding of enzyme to a trapping compound. However, the enzyme was not found to lose activity when incubated without template. Trapping by a DNA reaction product should be detected as enzyme-bound material. Yet when we isolated the enzyme-bound products and analyzed them by gel electrophoresis, no preferential affinity to any of the labeled products could be measured (data not shown). Furthermore, the enzyme-bound fraction did not decrease at later times; therefore, a substantial trapping of enzyme by

an unlabeled compound seems unlikely. These effects were observed for both primers, suggesting systematic deviation due to a reaction not taken into account by the model.

The experiments described were performed with RNA as template. When the extension experiments with primer 1 were repeated using instead the homologous DNA template (Figure 1), similar features were essentially observed (data not shown); in particular, pausing appeared to occur at the same position. The analysis confirmed the somewhat higher incorporation rates and extensibilities observed previously with RNA templates compared to those seen with DNA templates (Kati et al., 1992; Huber et al., 1989); a more thorough analysis with DNA as template would be expected to result in modification of some rate constants, but fundamental differences in the mechanism of pausing and fidelity seem unlikely.

DISCUSSION

The study we present was based on the steady-state kinetic gel assay developed in the group of M. F. Goodman (Boosalis et al., 1987; Goodman et al., 1993). The experimental results were compared with results from computer simulations, i.e. from the numerical integration of the rate equations using the mechanism and rate constants proposed (Figure 6, Tables 2 and 3). Our results show that the previously published kinetic mechanism (Kati et al., 1992; Hsieh et al., 1993) cannot adequately describe the multicycle extension of a primer−template by the polymerase activity of reverse transcriptase. Only when we extended this mechanism by introducing the two-step binding of enzyme to template (Divita et al., 1993; Rittinger et al., 1995; Jaju et al., 1995) did we obtain a satisfactory description; moreover, this was possible only by assuming that after each incorporation cycle the binary complex remains in its active, inner form. Another activation step at the end of each cycle, e.g. translocation, does not seem to be necessary; if it occurs, it does not contribute to the rates we have measured. In general, the published rate constants fitted the extension patterns well, except for the conversion of the inner complex into the outer one; to obtain a good fit both with our experiments and with the reported composite ${}^{i}k_{\mathrm{off}}$ value (0.11 s^{-1}; Hsieh et al., 1993), the rate constant for this reaction had to be adjusted to 0.2 s^{-1}. We also included the published rate for decomposition of the inactive ternary complex (Kati et al., 1992); however, the simulations showed that under our conditions this step did not contribute significantly to the total enzyme liberation rate.

We introduced the notion of extensibility, the probability that the extension proceeds at a certain position, to replace the similar notions of termination probability or specific processivity used in previous work, because the newly proposed quantity is conceptually and numerically easier to handle. Measured extensibility values were compatible with the calculated data only when the expanded mechanism (Figure 6) was used. When all four triphosphates were present at the relatively high concentration of 50 μM, we found an average processivity of 27 yet were able to account for the accumulation of intermediates without the unphysical assumption that the enzyme release rate is higher during consecutive incorporation cycles as compared to that during a single cycle (Kati et al., 1992). The average processivity we found is lower than that reported for poly(rA) template (90; Reardon et al., 1991), consistent with the observation that pausing is more pronounced on natural RNA templates than on homopolymers (Huber et al., 1989), but somewhat higher than the value of 10−20 obtained by Kati et al. (1992). It should be noted that pausing is usually not restricted to an isolated position; regions with higher or lower extensibilities, comprised of several bands, can be discerned (Figure 2). Since the measurements with primer 1 were done in a low-extensibility region, it is possible that the standard values need further readjustment when more data are available.

Site-specific changes of the standard rate constants were introduced to account for pausing. The rate constant adjustments were not done by fitting a single experiment, however. Changes of individual rate constants produced characteristic changes of the computed concentration profiles; these suggested which rate values had to be changed, and to approximately what extent, to obtain agreement with the experimental results. The parameters were then adjusted to obtain a satisfactory fit to all experimental data available. It resulted that the pausing at position 35 was mainly caused by an enhanced rate of reversion of the inner binary complex to the outer one, rather than by a low equilibrium constant for initial enzyme−template binding. It is likely that the formation of the outer complex merely involves electrostatic interactions between the binding site of the enzyme and the template, whereas the subsequent conversion to the inner complex involves conformational changes of both enzyme and template, leading to proper positioning and alignment (Patel et al., 1995); sequence-induced variations in the energy difference between the outer and inner complexes are plausible. The pause site at position 35 coincides with a site where, for extension to continue, a secondary structure of the RNA template probably has to be opened; this opening may be responsible for energy changes. On the other hand, pausing was also found to occur at positions where changes in the secondary structure of the template are not suggested by the sequence (Pop, 1996). Furthermore, about the same pausing at position 35 was observed also when using DNA as template, in which case the secondary structure is less stable. Similar pausing patterns at homologous RNA and DNA sequences have been observed by others (DeStefano et al., 1992). An additional contribution to the pausing at position 35 is provided by a reduced equilibrium constant for binding of the dNTP substrate to the inner complex. Since this binding is believed to involve proper base-pairing to the template (Johnson, 1993), it is conceivable that this process is impaired by the template base participating in a secondary interaction. For the subsequent step, i.e. activation of the ternary complex, modest adjustment of the rate constant value sufficed (Table 3) to bring calculation and experiment into agreement.

The simulations and the experiments both support a Michaelis−Menten formalism for dNTP substrate incorporation under single-hit, running-start conditions where a quasi-steady-state is achieved. However, despite the fact that the sensitivity analysis suggested correlations between ${}^{i}X$ and ${}^{i}K_{x}$ on one side and certain rate constants on the other, the model used does not lead to compact instructive analytical equations.

The discrimination coefficients found at both sites investigated were lower than expected. In this respect, the fact that both these sites are associated with pause effects may bear some significance. The kinetic analysis suggested that

the mechanisms responsible for misinsertion of dTTP at the two sites are different. Both steps of dNTP binding contribute to the discrimination against misinsertion (Johnson, 1993). At position 34, the binding equilibrium constant discriminates against dTTP by the unusually low factor of 40 (compared to the normal 200−400; Johnson, 1993), while the selectivity factor of 14 contributed by the second step (k_a) is in the normal range. At position 39, on the other hand, the discrimination factor in the first step (100) is close to normal, being unusually low in the second step (6). It seems plausible that dTTP misinsertion at position 34 is mainly due to transient misalignment (Kunkel & Alexander, 1986; Kunkel & Soni, 1988; Bebenek et al., 1993), the vicinity of template-^{35}A favoring the binding of dTTP. At position 39, where an adjacent A is missing, dTTP binding is not favored; the reason for the unusually low selectivity during the activation step is not clear.

Why are reverse transcriptases not processive enzymes like most other DNA and RNA polymerases? Intuitively, one would assume that processive polymerases accomplish their goal faster and thus have a selective advantage. The answer is not easy; other processes involved in the production of the provirus DNA, like strand transfer (DeStefano et al., 1994), might provide a selective advantage for a polymerase that frequently terminates and restarts synthesis.

ACKNOWLEDGMENT

We are indebted to Professor Roger Goody for the strain overproducing the HIV-1 reverse transcriptase, Professor Manfred Eigen for his interest and support, and Professor W. C. Gardiner for correcting our manuscript.

REFERENCES

Abbotts, J. M., Bebenek, K., Kunkel, T. A., & Wilson, S. H. (1993) *J. Biol. Chem. 268*, 10312−10323.
Aivazashvili, V. A., Bibilashvili, R. Sh., Vartikyan, R. M., & Kutateladze, T. V. (1981) *Mol. Biol. (Moscow) 15*, 653−667.
Bakhanashvili, M., & Hizi, A. (1993) *FEBS Lett. 319*, 201−205.
Bebenek, K., Abbotts, J., Wilson, S. H., & Kunkel, T. A. (1993) *J. Biol. Chem. 268*, 10324−10334.
Boosalis, M. S., Petruska, J., & Goodman, M. F. (1987) *J. Biol. Chem. 262*, 14689−14696.
DeStefano, J. J., Buiser, R. G., Mallaber, L. M., Fay, P. J., & Bambara, R. A. (1992) *Biochim. Biophys. Acta 1131*, 270−280.
DeStefano, J. J., Bambara, R. A., & Fay, P. J. (1994) *J. Biol. Chem. 269*, 161−168.
Divita, G., Müller, B., Immendörfer, U., Gautel, M., Rittinger, K., Restle, T., & Goody, R. S. (1993) *Biochemistry 32*, 7966−7971.
Fersht, A. R. (1985) *Enzyme Structure and Mechanism*, W. H. Freeman, New York.
Goodman, M. F., Creighton, S., Bloom, L. B., & Petruska, J. (1993) *Crit. Rev. Biochem. Mol. Biol. 28*, 83−126.
Gopalakrishnan, V., Peliska, J. A., & Benkovic, S. J. (1992) *Proc. Natl. Acad. Sci. U.S.A. 89*, 10763−10767.
Hsieh, J.-C., Zinnen, S., & Modrich, P. (1993) *J. Biol. Chem. 268*, 24607−24613.
Huber, H. E., McCoy, J. M., Seehra, J. S., & Richardson, C. C. (1989) *J. Biol. Chem. 264*, 4669−4678.
Jaju, M., Beard, W. A., & Wilson, S. H. (1995) *J. Biol. Chem. 270*, 9740−9747.
Johnson, K. A. (1993) *Annu. Rev. Biochem. 62*, 685−713.
Kati, W. M., Johnson, K. A., Jerva, L. F., & Anderson, K. S. (1992) *J. Biol. Chem. 267*, 25988−25997.
Klarmann, G. J., Schauber, C. A., & Preston, B. D. (1993) *J. Biol. Chem. 268*, 9793−9802.
Kunkel, T. A., & Alexander, P. S. (1986) *J. Biol. Chem. 261*, 160−166.
Kunkel, T. A., & Soni, A. (1988) *J. Biol. Chem. 263*, 14784−14789.
Mills, D. R., Dobkin, C., & Kramer, F. R. (1978) *Cell 15*, 541−550.
Müller, B., Restle, T., Weiss, S., Gautel, M., Sczakiel, G., & Goody, R. (1989) *J. Biol. Chem. 264*, 13975−13978.
Patel, P. H., Jacobo-Molina, A., Ding, J. P., Tantillo, C., Clark, A. D., Raag, R., Nanni, R. G., Hughes, S. H., & Arnold, E. (1995) *Biochemistry 34*, 5351−5363.
Perrino, F. W., Preston, B. D., Sandell, L. L., & Loeb, L. A. (1989) *Proc. Natl. Acad. Sci. U.S.A. 86*, 8343−8347.
Pop, M. P. (1996) *Biochim. Biophys. Acta* (in press).
Reardon, J. E. (1993) *J. Biol. Chem. 268*, 8743−8751.
Reardon, J. E., Furfine, E. S., & Cheng, N. (1991) *J. Biol. Chem. 266*, 14128−14134.
Restle, T., Müller, B., & Goody, R. S. (1990) *J. Biol. Chem. 265*, 8986−8988.
Ricchetti, M., & Buc, H. (1990) *EMBO J. 9*, 1583−1593.
Rittinger, K., Divita, G., & Goody, R. S. (1995) *Proc. Natl. Acad. Sci. U.S.A. 92*, 8046−8049.
Sambrook, J., Fritsch, E. F., & Maniatis, T. (1989) *Molecular Cloning*, 2nd ed., Cold Spring Harbor Laboratory Press, Cold Spring Harbor, NY.
Smith, P. K., Krohn, R. I., Hermanson, G. T., Mallia, A. K., Gartner, F. H., Provenzano, M. D., Fujimoto, E. K., Goeke, N. M., Olson, B. S., & Klenk, D. C. (1985) *Anal. Biochem. 150*, 76−85.
Williams, K. J., & Loeb, L. A. (1992) *Curr. Topics Microbiol. Immunol. 176*, 165−180.
Yu, H., & Goodman, M. F. (1992) *J. Biol. Chem. 267*, 10888−10896.
Zinnen, S., Hsieh, J.-C., & Modrich, P. (1994) *J. Biol. Chem. 269*, 24195−24202.
Zuker, M., & Stiegler, P. (1981) *Nucleic Acids Res. 9*, 133−148.

BI9530292